

Submillimeter-wave spectroscopy of VN ($X^3\Delta_r$) and VO ($X^4\Sigma^-$): A study of the hyperfine interactions

M.A. Flory, L.M. Ziurys *

Departments of Chemistry and Astronomy, Steward Observatory, University of Arizona, 933 N. Cherry Ave., Tucson, AZ 85721, USA

Received 4 July 2007; in revised form 13 September 2007

Available online 26 September 2007

Abstract

The pure rotational spectra of VN ($X^3\Delta_r$) and VO ($X^4\Sigma^-$) have been recorded in the frequency range 290–520 GHz using direct absorption spectroscopy. These radicals were synthesized in the gas-phase from the reaction of VCl_4 with either N_2 or H_2O in an AC discharge. Seven rotational transitions were recorded for each molecule; in both sets of spectra, fine and hyperfine structures were resolved. The data sets for VN and VO were fit with Hund's case (a) and case (b) Hamiltonians, respectively, and rotational, fine structure, and hyperfine constants determined. For VN, however, an additional hyperfine parameter, Δa , was necessary for the analysis of the $\Omega = 2$ sublevel to account for perturbations from a nearby $^1\Delta$ state, in addition to the usual Frosch and Foley constants. Determination of Δa suggests that the $^1\Delta$ state lies $\sim 3000\text{ cm}^{-1}$ above the ground state. In VO, the hyperfine structure in the F_2 and F_3 components was found to become heavily mixed due to an avoided crossing, predicted by previous optical studies to be near the $N = 15$ level. The hyperfine constants established for these two molecules are consistent with the proposed $\sigma^1\delta^1$ and $\sigma^1\delta^2$ electron configurations.
© 2007 Elsevier Inc. All rights reserved.

Keywords: Rotational spectroscopy; Transition metals; Hyperfine; Bonding; VN; VO

1. Introduction

Spectroscopy of small vanadium compounds in the gas-phase is relevant for a variety of applications. For example, such data may be useful in identifying atmospheric contaminants containing this element in urban areas [1]. Electronic spectra of VO have been found in the atmospheres of cool stars, and V-containing compounds were recently discovered in comet nuclei [2,3], generating an astrophysical interest. In addition, important aspects of chemical bonding in this element can be deduced from spectroscopic studies. Unfortunately, only a limited number of vanadium-containing species have been investigated spectroscopically to date at any resolution; these species include VN, VO, VF, VS, VCl, VCl^+ , and VCH [4–10]. Of these species, only three have been studied by rotational methods. The lowest transitions of VO have been recorded using

FTMW techniques [11], and very recently, submillimeter studies of VCl and VCl^+ have been carried out [9,12].

The first gas-phase study of VN was carried out by Simard et al., who investigated the $d^1\Sigma^+-X^3\Delta$ transition using laser-induced fluorescence (LIF) techniques [13]. Following this work, Balfour et al. conducted a LIF study of the $D^3\Pi-X^3\Delta_r$ transition with sufficient resolution to observe the hyperfine structure in both electronic states [4]. These authors only established the hyperfine parameters for individual Ω ladders, however, because of perturbations from other nearby states. In addition, Ram et al. have investigated the $a^1\Delta$, $b^1\Sigma^+$, $d^1\Sigma^+$, $e^1\Pi$, and $f^1\Phi$ states of VN using Fourier transform spectroscopy in the near infrared region [14,15].

Laboratory spectroscopy of VO dates back to at least 1968, with the work of Richards and Barrow, who investigated a $^4\Sigma^--X^4\Sigma^-$ electronic transition [16]. These authors discovered that the hyperfine structure in the ground electronic state underwent an internal perturbation because of an avoided crossing. Optical studies of the

* Corresponding author. Fax: +1 520 621 5554.

E-mail address: lziurys@as.arizona.edu (L.M. Ziurys).

$B^4\Pi-X^4\Sigma^-$, $A^4\Pi-X^4\Sigma^-$, $C^4\Sigma^-X^4\Sigma^-$, and ${}^2\Phi-1^2\Delta$ transitions of VO were subsequently conducted [5,17–19], followed by Fourier transform microwave spectroscopy of the $N=0 \rightarrow 1$, $J=3/2 \rightarrow 1/2$ transition near 8 GHz [11]. In 1995, Adam et al. determined the most accurate set of spectroscopic constants for the ground state to date by combining the microwave data with LIF measurements of the $B^4\Pi-X^4\Sigma^-$ transition [5].

In this paper, we present measurements of the submillimeter spectra of the VN ($X^3\Delta_r$) and VO ($X^4\Sigma^-$) radicals in their ground vibrational states. As expected from past work, perturbations were found in the hyperfine structure for both radicals in these pure rotational data. From these measurements, improved spectroscopic constants have been established for the two species. Here, we present our results, subsequent analysis, and interpretation of the hyperfine parameters.

2. Experimental

The spectra of the VN and VO radicals were recorded using the velocity modulation spectrometer of the Ziurys group, which has been described in detail elsewhere [20,21]. Briefly, the radiation source consists of Gunn oscillator/Schottky diode multiplier combinations that provide nearly continuous frequency coverage from 65 to 660 GHz. The reaction chamber is a single-pass, glass cell cooled to -65°C with chilled methanol. Ring electrodes are located at each end of the cell to support an AC discharge. An InSb hot-electron bolometer serves as the detector. For this study, the spectrometer was used solely in source modulation mode as a direct absorption system (see Ref. [21]), and signals are detected at $2f$ using a lock-in amplifier.

Vanadium nitride was produced using 1 mTorr of VCl_4 , 3–5 mTorr of N_2 , and 20 mTorr of Ar in the AC discharge with a power level of 250 W. The plasma created in the discharge glowed a deep purple, likely due to vanadium atomic emission. In searching for VN, vanadium oxide signals were observed without addition of any extra gases, likely a result of residual water. Rotational transitions of VCl and VCl^+ were also observed.

Transition frequencies for VN were predicted based on the constants of Balfour et al. [4], and a search range of several hundred MHz was carried out to locate all three spin components. Most transitions, but not all, were observed within 15–20 MHz of the predicted frequency. For VO, predicted transitions based on the constants of Adam et al. were typically accurate to 5–10 MHz [5] and required less scanning. After the correct patterns were identified, transition frequencies for both species were measured by averaging two scans, one taken to increasing frequency and one to decreasing frequency, each 5 MHz in width. The line shapes were fit with Gaussian profiles to establish the center positions, and line widths ranged from 0.5 to 1.2 MHz over the range 300–520 GHz. The experimental accuracy for these data is estimated to be ± 50 kHz.

3. Results and analysis

The observed rotational frequencies for VN ($X^3\Delta_r$) are listed in Table 1. Seven rotational transitions were measured, spanning the frequency range 297–528 GHz. Each rotational transition is split into three fine structure components ($\Omega = 1, 2$, and 3), which are further divided into eight hyperfine lines owing to the vanadium nuclear spin ($I = 7/2$). No evidence of A -doubling was observed in these spectra, and hyperfine interactions from the nitrogen nucleus were also not seen. These results are consistent with the findings of Balfour et al. [4]. In total, 159 lines were measured and included in the final analysis.

Fig. 1 shows sample spectra of the three spin components of VN in the $J = 12 \leftarrow 11$ transition. In each case, the octet pattern resulting from vanadium hyperfine interactions is clearly apparent. Although not discernable from the figure, the frequency spacing of the three fine structure components is fairly even, indicative of strong Hund's case (a) coupling. It is clear from Fig. 1 that the ordering of the hyperfine components is reversed in frequency in the $\Omega = 1$ ladder relative to the $\Omega = 2$ and 3 sub-states. Also, the hyperfine structure of the $\Omega = 3$ component is spaced considerably wider in frequency than in the two other ladders. For example, while the $\Omega = 1$ hyperfine pattern spans 120 MHz, the $\Omega = 3$ spectrum covers over 350 MHz.

The transitions recorded for VO in its $X^4\Sigma^-$ state are presented in Table 2. Seven rotational transitions, each consisting of four spin components, have been measured in the frequency range 291–525 GHz. However, in the F_1 and F_4 states ($J = N + 3/2$, $J = N - 3/2$), the hyperfine pattern is such that many components are blended and could not be satisfactorily used in the analysis. Therefore, only 188 spectral lines could be included in the fit.

Sample spectra of VO are presented in Fig. 2. Here, each of the four spin components of the $N = 12 \leftarrow 11$ rotational transition is individually shown, with the vanadium hyperfine structure clearly apparent. However, none of these data exhibit hyperfine structure that follows the classic Landé-like pattern, as seen for VN. Instead, the hyperfine lines of each spin component reverse in frequency midway through the pattern and form a “bandhead,” particularly prominent in the F_2 and F_3 data. Although not evident in the spectra, the eigenvectors for the hyperfine levels in the F_2 and F_3 states become highly mixed and contribute to this reversal. This behavior was noted by both Cheung et al. [17] and Adam et al. [5] in their optical data and was attributed to internal hyperfine perturbations due to an avoided crossing of the F_2 and F_3 spin levels near $N = 15$. The mixing of levels follows the selection rules $\Delta N = 0$, $\Delta J = 1$, and $\Delta F = 0$. The F_2 , $F = J + 7/2$ and F_3 , $F = J - 7/2$ levels remain unperturbed because they cannot connect to the other spin component by the selection rule $\Delta F = 0$. These unperturbed transitions appear separate from the “bandhead” pattern and are identified in Fig. 2 by the dagger symbol. The F_1 and F_4 groups also show a bandhead-type structure but over a smaller frequency range,

Table 1
Observed rotational transition frequencies of VN ($X^3\Delta_1; v=0$)^a

$J+1$	$F+1$	←	J	F	$\Omega=1$		$\Omega=2$		$\Omega=3$	
					ν	$\nu_{\text{obs-calc}}$	ν	$\nu_{\text{obs-calc}}$	ν	$\nu_{\text{obs-calc}}$
8	4.5		7	3.5	297223.514	0.018	300198.223	0.007		
	5.5			4.5	297238.156	0.015	300190.129	0.000		
	6.5			5.5	297255.085	0.004	300175.698	0.096		
	7.5			6.5	297274.346	-0.008	300154.693	0.022		
	8.5			7.5	297296.031	0.018	300127.402	0.017		
	9.5			8.5	297320.119	-0.006	300093.822	0.018		
	10.5			9.5	297346.755	-0.016	300053.989	-0.014		
	11.5			10.5	297376.069	0.023	300008.068	-0.002		
9	5.5		8	4.5	334380.429	0.009	337669.733	0.042	340400.362	0.006
	6.5			5.5	334395.153	-0.001	337661.315	0.021	340365.574	-0.026
	7.5			6.5	334411.468	-0.020	337648.388	-0.003	340314.572	-0.006
	8.5			7.5	334429.447	-0.005	337631.000	-0.010	340247.727	0.338
	9.5			8.5	334449.105	0.021	337609.168	-0.018	340164.145	-0.010
	10.5			9.5	334470.431	-0.002	337582.985	0.023	340065.024	-0.006
	11.5			10.5	334493.545	-0.012	337552.395	0.004	339950.220	0.031
	12.5			11.5	334518.531	0.010	337517.531	-0.001	339819.787	-0.055
10	6.5		9	5.5	371529.747	0.006	375141.693	0.011	378106.256	-0.032
	7.5			6.5	371544.366	-0.002	375133.522	0.022	378072.341	-0.004
	8.5			7.5	371560.148	-0.004	375122.030	-0.012	378026.580	-0.020
	9.5			8.5	371577.104	-0.013	375107.298	-0.031	377969.145	0.015
	10.5			9.5	371595.296	0.003	375089.379	-0.010	377900.033	0.008
	11.5			10.5	371614.720	0.003	375068.253	0.000	377819.413	0.019
	12.5			11.5	371635.433	0.002	375043.946	-0.013	377727.354	-0.010
	13.5			12.5	371657.483	-0.002	375016.554	0.004	377624.075	-0.003
11	7.5		10	6.5	408671.780	-0.012	412611.044	-0.010	415820.354	-0.021
	8.5			7.5	408686.222	-0.011	412603.310	0.020	415788.038	0.055
	9.5			8.5	408701.517	-0.019	412593.060	-0.010	415746.775	0.016
	10.5			9.5	408717.725	0.004	412580.405	-0.006	415696.759	-0.003
	11.5			10.5	408734.810	-0.001	412565.196	-0.138	415638.079	0.019
	12.5			11.5	408752.847	0.011	412547.856	-0.006	415570.753	0.021
	13.5			12.5	408771.823	-0.004	412528.020	-0.003	415494.922	0.053
	14.5			13.5	408791.833	0.009	412505.929	0.077	415410.632	0.059
12	8.5		11	7.5	445807.533	1.007 ^b	450075.678	-0.014	453536.651	-0.004
	9.5			8.5	445820.743	-0.012	450068.390	-0.020	453506.030	-0.004
	10.5			9.5	445835.625	-0.018	450059.225	-0.014	453468.623	-0.011
	11.5			10.5	445851.187	-0.017	450048.192	0.000	453424.499	-0.001
	12.5			11.5	445867.465	0.006	450035.286	-0.001	453373.662	-0.020
	13.5			12.5	445884.445	0.014	450020.549	0.008	453316.236	-0.004
	14.5			13.5	445902.148	0.002	450003.992	0.014	453252.225	-0.017
	15.5			14.5	445920.628	-0.006	449985.625	0.004	453181.708	-0.054
13	9.5		12	8.5	482933.677	-0.017	487534.032	-0.002	491251.162	-0.016
	10.5			9.5	482947.709	0.000	487527.231	-0.002	491222.375	0.054
	11.5			10.5	482962.258	0.021	487518.939	-0.010	491188.143	-0.006
	12.5			11.5	482977.303	0.013	487509.160	-0.031	491148.710	0.015
	13.5			12.5	482992.874	-0.011	487497.970	-0.005	491103.999	0.000
	14.5			13.5	483009.023	-0.018	487485.311	-0.003	491054.099	-0.008
	15.5			14.5	483025.758	-0.022	487471.236	0.010	490999.052	-0.016
	16.5			15.5	483043.139	0.014	487455.758	0.027	490938.921	-0.017
14	10.5		13	9.5	520052.943	0.015	524984.906	0.077	528961.114	-0.027
	11.5			10.5	520066.751	0.014	524978.508	0.025	528933.965	0.019
	12.5			11.5	520080.954	0.003	524970.925	-0.026	528902.495	-0.011
	13.5			12.5	520095.595	0.013	524962.222	-0.019	528866.871	0.023
	14.5			13.5	520110.651	0.008	524952.354	-0.011	528827.013	0.009
	15.5			14.5	520126.159	0.009	524941.326	-0.008	528782.998	-0.009
	16.5			15.5	520142.112	-0.011	524929.152	-0.011	528734.880	-0.018
	17.5			16.5	520158.568	-0.011	524915.892	0.024	528682.727	0.010

^a In MHz.

^b Blended line; not included in fit.

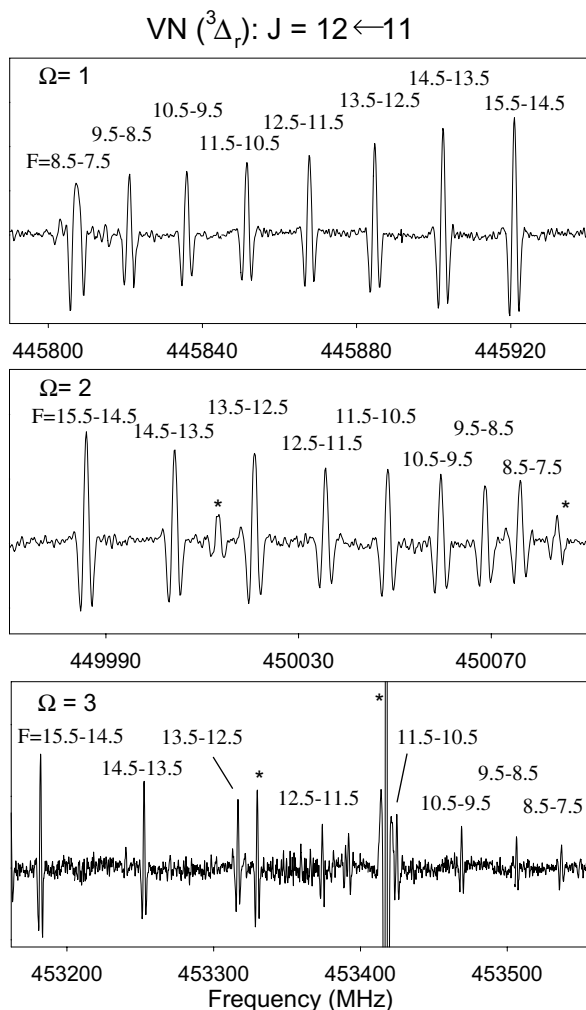


Fig. 1. Representative spectra of VN ($X^3\Delta_r$) in the $J = 12 \leftarrow 11$ rotational transition near 450 GHz. Each panel displays one of the three fine structure components, labeled by Ω in a Hund's case (a) scheme, which are each further split into hyperfine octets by the vanadium nuclear spin ($I = 7/2$). Individual hyperfine components are indicated by quantum number F . Unidentified lines are marked with an asterisk. Variations are seen in the three patterns. The hyperfine ordering increases with frequency for the $\Omega = 1$ data, while it decreases for the other two components. The $\Omega = 3$ data also extend over a much larger frequency range relative to the other two patterns. The top panel is a composite of two scans, each 75 MHz wide and recorded in 60 s. The middle graph is from a single scan, 120 MHz wide, acquired in 90 s. The bottom plot is composed of four, 100 MHz scans, each with a 60 s scan time.

which causes blending of some of the hyperfine components. Even though these levels cross near $N = 8$, the F_1 and F_4 components differ by $\Delta J = 3$ and cannot perturb one another. Moreover, no mixing of levels was evident in the eigenvectors when fitting the F_1 and F_4 spectra. The pattern in this case is simply a result of the approximate diagonal case (b) matrix element:

$$\pm \frac{3}{2} [F(F+1) - J(J+1) - I(I+1)] * [b_F/R(N)], \quad (1)$$

where the + and - (and $R(N) = 2N+3$ and $R(N) = 2N-1$) correspond to F_1 and F_4 , respectively. This term produces a reversal of the hyperfine pattern as the F quantum number increases relative to J , N and I .

Spectroscopic parameters for vanadium nitride were obtained using an effective Hund's case (a) Hamiltonian of the form:

$$H_{\text{eff}} = H_{\text{rot}} + H_{\text{so}} + H_{\text{ss}} + H_{\text{mhf}} + H_{\text{eq}Q}. \quad (2)$$

The terms here account for molecular frame rotation, electron spin-orbit coupling, electron spin-spin coupling, and magnetic hyperfine and electric quadrupole effects from the vanadium nucleus, including a modification to the regular case (a_β) matrix elements. The hyperfine structure was fit using the usual Frosch and Foley terms a , b , and $(b+c)$, as well as the electric quadrupole parameter eqQ . In addition, a perturbation term Δa had to be included to obtain a global fit. As has been noted by Balfour et al., the hyperfine structure of the $\Omega = 2$ level in the $X^3\Delta_r$ state experiences a perturbation due to isoconfigurational mixing with the $^1\Delta$ excited state [4], producing a cross term between the spin-orbit and Fermi contact Hamiltonians [22]. The main consequence of this perturbation is to modify the value of a . Because of this effect, an additional parameter, Δa , was included in the Hamiltonian for the $\Omega = 2$ diagonal matrix element, which takes the modified form:

$$\frac{[aA + \Delta a + (b+c)\Sigma]\Omega[F(F+1) - J(J+1) - I(I+1)]}{2J(J+1)}. \quad (3)$$

(The usual expression for the matrix element is $aA + (b+c)\Sigma$, with $A = 2$ and $\Sigma = 0$.) In addition to Δa , centrifugal distortion corrections to several of the parameters were also employed, including A_D , λ_D , λ_H , and $(b+c)_D$. All parameters were allowed to vary in the final fit. The resulting spectroscopic constants are given in Table 3 along with the values determined by Balfour et al. [4]. The rms of the fit is 23 kHz.

The VO data were fit using a Hund's case (b) effective Hamiltonian (N^2 representation):

$$H_{\text{eff}} = H_{\text{rot}} + H_{\text{sr}} + H_{\text{ss}} + H_{\text{mhf}} + H_{\text{eq}Q}. \quad (4)$$

The Frosch and Foley hyperfine parameters b_F and c were used, as well as the nuclear spin-rotation interaction term, C_I , in a $b_{\beta J}$ coupling scheme. Centrifugal distortion terms were included for rotational and spin interactions. Because $S > 1$, the third-order spin-rotation term, γ_s , and the third-order spin-orbit distortion to the Fermi contact interaction, b_s , were also included [17]. The F_1 and F_4 transition frequencies were fit with the above Hamiltonian with no modification. However, the avoided crossing of the F_2 and F_3 states near $N = 15$ causes these levels to mix. As a consequence, the quantum number labels (eigenvectors) lose their meaning in the region near the perturbation. To fit the data, therefore, the values of the F quantum numbers had to be fixed. The three low- J transitions measured in the microwave region by Suenram et al. [11] were also included in the fit. The resulting spectroscopic

Table 2
Observed rotational transition frequencies of VO ($X^4\Sigma^-; v = 0$)^a

N'	F'	←	N''	F''	$F_4 (J'' = N'' - 3/2)$		F'	←	F''	$F_3 (J'' = N'' - 1/2)$		F'	←	F''	$F_2 (J'' = N'' + 1/2)$		F'	←	F''	$F_1 (J'' = N'' + 3/2)$		
					ν	$\nu_{\text{obs-calc}}$				ν	$\nu_{\text{obs-calc}}$				ν	$\nu_{\text{obs-calc}}$				ν	$\nu_{\text{obs-calc}}$	
0	3		1	3			8584.434 ^b				0.008											
	4			3			10983.309 ^b				-0.003											
	5			4			8742.411 ^b				0.003											
9	4		8	3	291860.801	0.172	5	4	293722.745	0.024	6	5	296266.224	-0.070	7	6	296368.049	-0.509 ^c				
	5			4	291780.859	0.030	6	5	293739.109	-0.011	7	6	296245.767	-0.041	8	7	296402.330	-0.047				
	6			5	291716.282	0.035	7	6	293750.243	-0.007	8	7	296225.376	-0.026	9	8	296425.123	-0.104				
	7			6	291666.659	0.066	8	7	293755.008	-0.031	9	8	296206.913	-0.007	10	9	296437.219	0.221 ^c				
	8			7	291631.483	0.028	9	8	293752.100	-0.018	10	9	296193.378	0.026	11	10	296437.658	0.126 ^c				
	9			8	291610.349	0.039	10	9	293739.109	0.023	11	10	296190.751	0.134	12	11	296426.603	-0.029				
	10			9	291602.584	0.058	11	10	293710.752	0.028	12	11	296212.942	-0.027	13	12	296404.022	-0.032				
	11			10	291607.419	0.025	12	11	293653.630	0.054	13	12	296305.960	-0.040	14	13	296369.482	-0.017				
10	5		9	4	325054.643	0.038	6	5	326577.527	-0.005	7	6	328762.810	-0.003	8	7	329021.620	-0.305 ^c				
	6			5	324991.938	0.000	7	6	326606.107	-0.046	8	7	328730.692	-0.052	9	8	329050.263	0.295 ^c				
	7			6	324942.315	-0.003	8	7	326629.529	-0.048	9	8	328700.203	0.018	10	9	329069.066	0.206 ^c				
	8			7	324905.508	-0.009	9	8	326646.815	-0.039	10	9	328672.780	-0.020	11	10	329078.641	0.138 ^c				
	9			8	324881.189	-0.040	10	9	326656.753	0.059	11	10	328651.530	-0.034	12	11	329078.641	-0.132 ^c				
	10			9	324868.951	-0.136 ^c	11	10	326656.653	0.074	12	11	328643.093	-0.043	13	12	329069.366	-0.135 ^c				
	11			10	324868.751	0.096	12	11	326640.405	0.024	13	12	328666.370	-0.024	14	13	329050.363	-0.126 ^c				
	12			11	324879.438	0.006	13	12	326589.827	0.003	14	13	328802.908	-0.041	15	14	329021.620	0.126 ^c				
11	6		10	5	358100.453	0.092	7	6	359401.883	-0.004	8	7	361312.470	-0.034	9	8	361687.990	0.135 ^c				
	7			6	358050.068	-0.012	8	7	359445.851	-0.003	9	8	361266.787	-0.038	10	9	361711.360	-0.102				
	8			7	358010.929	0.014	9	8	359483.619	-0.061	10	9	361224.211	-0.057	11	10	361727.391	0.062				
	9			8	357982.658	-0.025	10	9	359514.835	-0.009	11	10	361185.924	-0.020	12	11	361735.402	0.036				
	10			9	357965.261	0.109	11	10	359538.492	-0.046	12	11	361154.352	0.092 ^c	13	12	361735.402	-0.061				
	11			10	357958.116	0.081	12	11	359552.771	0.052	13	12	361135.699	-0.018	14	13	361727.391	-0.092				
	12			11	357961.064	0.049	13	12	359551.242	-0.061	14	13	361152.951	-0.077	15	14	361711.260	0.002				
	13			12	357973.708	-0.023	14	13	359512.071	0.023	15	14	361360.953	-0.031	16	15	361686.538	-0.052				

12	7	11	6	391051.222	0.064	8	7	392202.263	-0.006	9	8	393892.910	-0.034	10	9	394361.628	0.071
	8		7	391010.039	0.001	9	8	392267.004	-0.018	10	9	393830.088	-0.004	11	10	394381.352	-0.344 ^c
	9		8	390978.438	0.020	10	9	392322.795	-0.001	11	10	393772.727	-0.015	12	11	394395.112	-0.088
	10		9	390956.269	0.123	11	10	392370.285	-0.010	12	11	393720.622	-0.020	13	12	394401.989	-0.004
	11		10	390943.134	0.100	12	11	392410.018	-0.007	13	12	393674.524	-0.002	14	13	394401.989	0.010
	12		11	390938.873	0.011	13	12	392441.552	0.004	14	13	393638.476	-0.015	15	14	394395.112	0.071
	13		12	390943.334	-0.048	14	13	392461.114	0.010	15	14	393632.676	-0.014	16	15	394381.152	0.114 ^c
	14		13	390956.269	-0.050	15	14	392448.966	0.048	16	15	393957.987	-0.015	17	16	394359.755	-0.050
14	9	13	8	456777.977	-0.028	10	9	457747.069	0.002	11	10	459080.143	0.026	12	11	459719.177	0.103 ^c
	10		9	456749.142	-0.028	11	10	457888.525	-0.069	12	11	458968.290	-0.014	13	12	459734.126	-0.084 ^c
	11		10	456727.414	0.001	12	11	457994.882	0.191 ^c	13	12	458875.002	-0.019	14	13	459744.081	-0.242 ^c
	12		11	456712.606	-0.016	13	12	458080.408	-0.048	14	13	458791.104	0.009	15	14	459749.320	-0.032 ^c
	13		12	456704.695	0.025	14	13	458155.229	-0.012	15	14	458708.981	0.001	16	15	459749.320	0.096
	14		13	456703.409	0.001	15	14	458226.775	-0.029	16	15	458619.034	-0.021	17	16	459744.081	0.230 ^c
	15		14	456708.663	-0.013	16	15	458305.047	0.049	17	16	458497.692	-0.034	18	17	459733.530	0.399 ^c
	16		15	456720.275	-0.023	17	16	458413.712	0.037	18	17	459217.926	0.002	19	18	459716.916	-0.026 ^c
15	10	14	9	489583.920	0.047	11	10	490496.383	-0.001	12	11	491654.191	0.061	13	12	492398.544	0.402 ^c
	11		10	489559.234	-0.017	12	11	490712.115	-0.024	13	12	491516.371	0.028	14	13	492411.988	0.545 ^c
	12		11	489540.757	-0.049	13	12	490844.770	-0.017	14	13	491410.961	0.047	15	14	492420.277	-0.039 ^c
	13		12	489528.447	0.005	14	13	490943.600	0.015	15	14	491318.445	0.015	16	15	492424.652	-0.057 ^c
	14		13	489521.986	-0.064	15	14	491028.111	0.004	16	15	491207.912	0.033	17	16	492424.652	0.096 ^c
	15		14	489521.586	0.080	16	15	491119.468	-0.003	17	16	491226.246	-0.015	18	17	492419.877	0.096 ^c
	16		15	489526.657	-0.017	17	16	491111.205	0.045	18	17	491354.613	0.074	19	18	492410.490	0.197 ^c
	17		16	489537.391	-0.019	18	17	490961.978	-0.027	19	18	491865.342	0.025	20	19	492395.984	-0.003 ^c
16	11	15	10	522362.559	0.028	12	11	523232.302	0.011	13	12	524191.270	0.059	14	13	525075.291	0.246 ^c
	12		11	522341.275	-0.004	13	12	523563.751	-0.072	14	13	524044.512	0.070	15	14	525087.489	0.666 ^c
	13		12	522325.106	-0.352	14	13	523705.940	-0.022	15	14	523942.044	0.031	16	15	525094.670	-0.001
	14		13	522314.877	-0.106	15	14	523802.501	-0.013	16	15	523883.888	0.016	17	16	525098.506	-0.035 ^c
	15		14	522309.717	-0.041	16	15	523853.738	0.071	17	16	523965.145	0.061	18	17	525098.506	0.130 ^c
	16		15	522309.717	0.037	17	16	523764.506	-0.006	18	17	524061.202	0.022	19	18	525094.370	0.263 ^c
	17		16	522314.677	0.045	18	17	523659.675	-0.015	19	18	524202.160	0.071	20	19	525086.110	0.454 ^c
	18		17	522324.506	0.012	19	18	523509.454	-0.004	20	19	524517.745	0.010	21	20	525072.849	-0.081 ^c

^a In MHz.^b Data from Ref. [11].^c Blended line; not included in analysis.

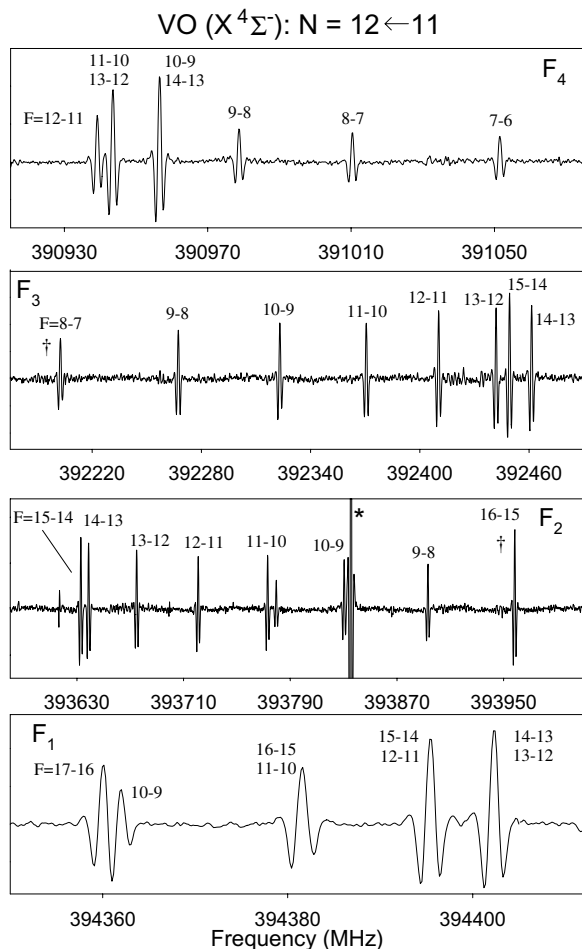


Fig. 2. Representative spectra of the $N = 12 \leftarrow 11$ rotational transition of $\text{VO} (X^4\Sigma^-)$ near 392 GHz. Each panel shows a single spin component, labeled F_1 through F_4 , which all exhibit vanadium hyperfine structure. Unidentified lines are marked with an asterisk. The hyperfine pattern in all four spin components reverses in frequency midway through the progression. Hence, in the F_1 and F_4 cases, some hyperfine components lie on top of each other. The F_2 and F_3 components also undergo an additional internal hyperfine perturbation, except for the $F = 8 \leftarrow 7$ and $F = 16 \leftarrow 15$ lines, which are marked by a dagger. The plots range from 80 to 430 MHz in width and are composites of single scans, 100 MHz in width, each acquired in 60 s.

constants are listed in Table 4, along with those of Adam et al. [5]. The overall rms of the fit is 52 kHz.

The constants from this analysis are in good agreement with previous work, except for the nuclear spin–orbit term b_s and the quadrupole coupling constant eqQ . In particular, the quadrupole constant derived here is negative ($eqQ = -2.5(1.5)$ MHz), while the optical value is larger and positive (40.2(4.8) MHz). In the Adam et al. study, however, C_1 was not used in the fit [5]. This difference, along with the use of a higher resolution data set, can account for these small discrepancies. It should be noted that a negative value of eqQ was also determined for NbO in its $X^4\Sigma^-$ state [23]. Both the niobium and vanadium nuclei have negative quadrupole moments; therefore, eqQ should be negative in the case of VO, as is found, additionally validating the analysis in this work.

Table 3
Spectroscopic constants for $\text{VN} (X^3\Delta_r)^a$

	Present work	Optical ^b
B	18 747.5574(12)	18 746.88(18)
D	0.0278342(36)	0.02729(31)
A	2 249 700(2900)	2 263 552(29)
A_D	-1.53(10)	-0.763(27)
λ	188 500(1100)	101 026.6(3.0)
λ_D	9.34(13)	-0.387(28)
λ_H	0.0002969(65)	
a	338.80(30)	
Δa	147.31(75)	
b	1350.8(2.9)	
$b + c$	1253.99(55)	
$(b + c)_D$	0.203(10)	
eqQ	15.9(2.3)	
h_1		1 940.3(8.4)
h_0		827.1(6.6)
h_{-1}		-586.4(9.0)
b_+		1321(83)
b_-		1404(57)
rms	0.023	138

^a In MHz; errors quoted are 3σ .

^b From Ref. [4].

Table 4
Spectroscopic constants for $\text{VO} (X^4\Sigma^-)^a$

	MM-wave ^b	Optical ^c
B	16 379.6186(14)	16 379.798(17)
D	0.0193638(39)	0.0194600(96)
γ	672.168(39)	672.328(42)
γ_D	0.001970(75)	0.001798(48)
γ_s	0.2204(81)	0.2427(95)
λ	60 881.03(55)	60 884.97(45)
λ_D	0.01816(61)	0.01145(68)
b_F	778.737(66)	777.54(15)
c	-129.84(19)	-134.83(46)
c_1	0.192 8(51)	
b_s	-0.660(14)	-0.472(37)
eqQ	-2.5(1.3)	40.2(4.8)
rms	0.052	11

^a In MHz; errors quoted are 3σ .

^b Includes current data and three frequencies from Ref. [11].

^c From Ref. [5].

4. Discussion

The vanadium hyperfine patterns in VN can be understood in terms of the derived constants, noting that $(b + c) > 2a$. These constants compete to generate the observed patterns, following the expression $h_\Sigma = aA + (b + c)\Sigma$. For $\Omega = 2$, $\Sigma = 0$, and the hyperfine pattern is entirely determined by the smaller $a + \Delta a$ value. When $\Omega = 1$ and $\Sigma = -1$, the term $(b + c)\Sigma$ reverses sign relative to aA , flipping the hyperfine structure into a rough mirror image of the $\Omega = 2$ pattern. For $\Omega = 3$, aA and $(b + c)\Sigma$ have the same sign (positive), leading in this case to a significantly larger splitting.

In the Balfour et al. work, five hyperfine parameters for the ground state of VN were established: $h_{\Sigma=1}$, $h_{\Sigma=0}$, and $h_{\Sigma=-1}$ (for the three spin components $\Omega = 1, 2,$ and 3), and two off-diagonal terms b_+ and b_- , which are coefficients for the elements $\langle \Sigma = 1 | H | \Sigma = 0 \rangle$ and $\langle \Sigma = 0 | H | \Sigma = -1 \rangle$, respectively [4]. These authors could not establish the individual Frosch and Foley parameters for either electronic state because of perturbations from the $a^1\Delta$, $d^1\Sigma^+$, and $e^1\Pi$ states. From the hyperfine parameters established here, h_1 , h_0 , and h_{-1} have been calculated for comparison with Balfour et al. The values derived are $h_1 = 1931.59(82)$, $h_0 = 824.91(56)$, and $h_{-1} = -576.39(82)$ MHz compared to $h_1 = 1940.3(8.4)$, $h_0 = 827.1(6.6)$, and $h_{-1} = -586.4(9.0)$ MHz—in complete agreement within the quoted uncertainties.

The additional hyperfine term Δa results from a perturbation by an excited $^1\Delta$ state [22]. This perturbation produces a cross-term between the spin–orbit and Fermi contact operators, $(\mathbf{L}\cdot\mathbf{S})(\mathbf{I}\cdot\mathbf{S})$, resulting in an effective $(\mathbf{I}\cdot\mathbf{L})$ interaction that changes the apparent value of a . From second-order perturbation theory, an expression for Δa can be derived [4]:

$$\Delta a = \frac{4A(b - c)}{\Delta E(^1\Delta - ^3\Delta)}, \quad (5)$$

where A is the spin–orbit constant of the $X^3\Delta_r$ state and $\Delta E(^1\Delta - ^3\Delta)$ is the energy difference between the $^1\Delta_2$ and $^3\Delta_2$ levels. Using the current hyperfine values, the energy of the excited $^1\Delta$ state is estimated to 2949 cm^{-1} above the $\Omega = 2$ level, or 3099 cm^{-1} above the ground state $^3\Delta_1$, slightly lower than the estimate of 3390 cm^{-1} by Balfour et al. [4]

No A -doubling was observed in VN up to $J = 15$ in any of the Ω ladders. In contrast, A -doubling was observed in the $\Omega = 1$ and 2 components in VF ($X^5\Delta_r$) [6], and very large A -doubling splittings have been measured for $\Omega = 0, 1, 2,$ and 3 in VCl ($X^5\Delta_r$) [12]. In the case of VCl, there are significant perturbations from nearby excited states lying at energies of approximately 500 cm^{-1} and 1600 cm^{-1} [24]. In VF, the interacting $^5\Pi$ state is 1700 cm^{-1} above the ground state [6]. In contrast, the lowest energy $^3\Pi$ state in VN has $\Delta E \approx 15000 \text{ cm}^{-1}$ [4], dramatically reducing A -doubling interactions. Lack of A -doubling splittings was also observed in the isoelectronic radical TiO ($X^3\Delta_r$) [25], suggesting that VN and TiO have similar electronic structures.

The proposed valence electron configurations of VN and VO are $\delta^1\sigma^1$ and $\delta^2\sigma^1$, respectively. Hence, these molecules differ in electronic structure by the presence of one δ electron. From the Fermi contact parameter, $b_F = b + c/3$, the amount of atomic vanadium $4s$ orbital character in the 9σ molecular orbital can be established in both species *via* the relationship:

$$\frac{b_F(\text{molecule})}{(1/2S)b_F(\text{atom})} \quad (6)$$

where S is the total spin. (The factor $(1/2S)$ arises because of differences in the microscopic vs. macroscopic form of the Hamiltonian for the Fermi contact interaction, namely $\langle S || s_i || S \rangle = (1/2S) \langle S || S || S \rangle$ [26].) The atomic b_F parameter for vanadium is 3105 MHz [27]. Hence, the 9σ orbital is approximately 84.9% and 75.2% V($4s$) in VN and VO, respectively, similar to the values derived by Balfour et al. [4]. Therefore, very little change in composition occurs in the 9σ orbital in going from VN to VO. On the other hand, there are two δ electrons in VO as opposed to only one in VN. This difference should affect the value of the c parameter because this constant is proportional to the angular factor $(3 \cos^2\theta - 1)$. While $s\sigma$ electrons contribute zero to this quantity, each $d\delta$ electron makes a contribution of $-4/7$. Thus, c should be a factor of 2 more negative in VO than VN, as is approximately found (-130 MHz vs. -97 MHz , respectively). The eqQ constant is proportional to the same angular factor, as well. This factor may also help explain the variation in the quadrupole parameter between VO and VN, which is small and negative in the oxide, and small but positive in the nitride.

5. Conclusions

Measurement of the submillimeter spectra of VO and VN has led to refined rotational, fine structure, and hyperfine constants. In particular, the Frosch and Foley hyperfine parameters for the vanadium nuclear spin in VN have been better determined. Both spectra show interesting patterns in their hyperfine structures, partly due to external and internal perturbations. Spectroscopic investigations of other vanadium compounds at high resolution would be useful for comparison.

Acknowledgments

The authors wish to thank J.M. Brown for use of his Hund's case (a) and case (b) fitting programs. This work was supported by NSF Grants CHE-04-11551 and CHE-07-18699.

References

- [1] S. Liiv, M. Kaasik, J. Atmospheric Chem. 49 (2004) 563.
- [2] M. Brett, Astron. Astrophys. 231 (1990) 440.
- [3] M.E. Zolensky et al., Science 314 (2006) 1735.
- [4] W.J. Balfour, A.J. Merer, H. Niki, B. Simard, P.A. Hackett, J. Chem. Phys. 99 (1993) 3288.
- [5] A.G. Adam, M. Barnes, B. Berno, R.D. Bower, A.J. Merer, J. Mol. Spectrosc. 170 (1995) 94.
- [6] R.S. Ram, P.F. Bernath, S.P. Davis, J. Chem. Phys. 116 (2002) 7035.
- [7] Q. Ran, W.S. Tam, A.S.-C. Cheung, A.J. Merer, J. Mol. Spectrosc. 220 (2003) 87.
- [8] R.S. Ram, P.F. Bernath, S.P. Davis, J. Chem. Phys. 114 (2001) 4457.
- [9] D.T. Halfen, L.M. Ziurys, in preparation.
- [10] M. Barnes, P.G. Hajigeorgiou, R. Kasrai, A.J. Merer, G.F. Metha, J. Am. Chem. Soc. 117 (1995) 2096.
- [11] R.D. Suenram, G.T. Fraser, F.J. Lovas, C.W. Gillies, J. Mol. Spectrosc. 148 (1991) 114.

- [12] D.T. Halfen, L.M. Ziurys, *J. Mol. Spectrosc.*, submitted for publication.
- [13] B. Simard, C. Masoni, P.A. Hackett, *J. Mol. Spectrosc.* 136 (1989) 44.
- [14] R.S. Ram, P.F. Bernath, S.P. Davis, *J. Mol. Spectrosc.* 210 (2001) 110.
- [15] R.S. Ram, P.F. Bernath, S.P. Davis, *J. Mol. Spectrosc.* 215 (2002) 163.
- [16] D. Richards, R.F. Barrow, *Nature* 219 (1968) 1244.
- [17] A.S.-C. Cheung, R.C. Hansen, A.J. Merer, *J. Mol. Spectrosc.* 91 (1982) 165.
- [18] A.S.-C. Cheung, A.W. Taylor, A.J. Merer, *J. Mol. Spectrosc.* 92 (1982) 391.
- [19] R.S. Ram, P.F. Bernath, S.P. Davis, A.J. Merer, *J. Mol. Spectrosc.* 211 (2002) 279.
- [20] C.S. Savage, L.M. Ziurys, *Rev. Sci. Instrum.* 76 (2005) 043106.
- [21] D.T. Halfen, L.M. Ziurys, *J. Mol. Spectrosc.* 234 (2005) 34.
- [22] Y. Azuma, J.A. Barry, M.P.J. Lyne, A.J. Merer, J.O. Schröder, J.L. Féménias, *J. Chem. Phys.* 91 (1989) 1.
- [23] A.G. Adam, Y. Azuma, J.A. Barry, A.J. Merer, U. Sassenberg, J.O. Schroeder, G. Cheval, J.L. Féménias, *J. Chem. Phys.* 100 (1994) 6240.
- [24] R.S. Ram, J. Liévin, P.F. Bernath, S.P. Davis, *J. Mol. Spectrosc.* 217 (2003) 186.
- [25] K. Namiki, S. Saito, J.S. Robinson, T.C. Steimle, *J. Mol. Spectrosc.* 191 (1998) 176.
- [26] T.D. Varberg, R.W. Field, A.J. Merer, *J. Chem. Phys.* 95 (1991) 1563.
- [27] W.J. Childs, O. Poulsen, L.S. Goodman, H. Crosswhite, *Phys. Rev. A* 19 (1979) 168.